IL NUOVO CIMENTO VOL. 23 C, N. 2 Marzo-Aprile 2000

Modelling study of mesoscale cyclogenesis over Ross Sea, Antarctica, on February 18, 1988

M. STORTINI, S. MORELLI (*) and S. MARCHESI ([1])

([1]) *Dipartimento di Scienze dell'Ingegneria, Sezione Osservatorio Geofisico Università di Modena e Reggio Emilia - Via Campi 213/A 41100, Modena, Italia*

(ricevuto il 23 Dicembre 1998; revisionato il 18 Gennaio 2000; approvato il 26 Gennaio 2000)

Summary. — This paper examines the development of a summer event of mesoscale cyclogenesis off the coast of Victoria Land in the presence of katabatic winds, by means of numerical simulations. These refer to the period from 00 UTC 17 February to 00 UTC 19 February 1988 and were performed using the hydrostatic ETA (1993 version) limited area model with resolution 55 km × 55 km × 17 levels. The ETA model reproduces katabatic winds from Terra Nova Bay and a trough on the southwestern Ross Sea. A cyclonic vortex is simulated in the trough, even though it is weaker than the one present in the analyses initialized by the European Center for Medium Range Weather Forecast (Reading, UK). Idealized simulations with varied surface conditions were also performed. In particular, an ice-covered ocean acts to weaken the atmospheric phenomena, while a no-mountain simulation emphasizes the influence of the orography and the cold winds from the coast of Victoria Land on the mesocyclonic activity.

PACS 92.60 – Meteorology.
PACS 93.30.Ca – Antarctica.
PACS 92.60.Gn – Winds and their effects.

1. – Introduction

Limited area models have been used for meteorological simulations of various area of the globe with good results. Recently, Hines *et al.* [1] have run a mesoscale model (MM4) using initial and boundary conditions provided by the European Centre for Medium Range Weather Forecast (ECMWF), for a period of 1 month (June 1988) for the whole of Antarctica. The continent is unique in various aspects. Antarctica is the Earth's highest and coldest continent: over 60% of its surface is situated above 2000 m in elevation and nearly 30% above 3000 m. On most of the interior ice plateau the slope of the surface is very small; by contrast, the gradient increases rapidly near the coast,

(*) E-mail: morelli@unimo.it

such that the orography rises over 1000 m in the space of 50 km. The katabatic winds, well known for their high directional constancy, and the low surface temperatures are perhaps the most characteristic features of Antarctic climatology [2, 3]. Near the coast, where the slopes are steep, the flows are channeled by the orography and converge at high speed into narrow confluence areas. Previous studies [4, 5] have identified many confluence zones; Adelie Land and Terra Nova Bay (TNB) are some of the best-known regions. Bromwich [6] has pointed out that mesoscale cyclogenesis seems to be associated with continental katabatic air stream, and that in the region adjacent to TNB mesoscale cyclones form with great frequency. Gallée [7] has shown that katabatic winds could play an important role in the formation and deepening of southwestern Ross Sea mesocyclones. Moreover, Bromwich and Kurtz [8] found that the polynya formation in TNB is mainly due to the forcing of katabatic wind on the coastal pack ice. A crucial point is the interaction air-sea-ice and the thermal and mechanical energy exchange at the surface-atmosphere interface. These considerations suggest the importance of the use of mesoscale numerical models in integrating the scant observations into a coherent picture of the Antarctic atmospheric flow. The model used in this study is the ETA model (now operational at NCEP, National Center for Environmental Prediction, Washington DC, USA). With varying resolutions and integration domain sizes, the model has also been implemented over Europe [9, 10] with good results, but it has never been run in the Antarctic region. The main goal of this paper is to study a mesoscale cyclogenesis that occurred in February 1988 off the coast of Victoria Land [11] by means of numerical simulations initialized with real data, and to examine the impact of changing the specifications of surface conditions. A description of the ETA model is given in sect. **2**. Comparison between ETA simulations from 17 to 19 February 1988 and ECMWF analyses is presented in sect. **3**. Three numerical experiments will be described. The first is the so-called control simulation hereafter referred to as CS; the second is a no-mountain experiment, referred to as NM; in the last one, referred to as SI, it is assumed that the ocean surface surrounding the continent is covered with ice up to 70° S in order to examine the influence of sea-ice cover on mesocyclonic activity. Conclusions and future developments are presented in sect. **4**.

2. – Model description and characteristics of the run

The mesoscale ETA model used in the simulations presented here is a three-dimensional (3D) hydrostatic primitive equation model described in detail by Black [12], Lazic and Telenta [13], and Mesinger *et al.* [14]. The semistaggered Arakawa E grid, which is the basis of the model's horizontal structure, lies upon a rotated latitude-longitude framework. This transformed coordinates system is created by rotating the Earth's geographic latitude-longitude grid so as to place the intersection of the equator and the prime meridian over the centre of the integration domain. In this way the convergence of the meridians is minimized over this area and a more uniform grid is obtained, particularly at higher latitudes. The grid resolution currently used is about 55 km at the centre of domain (74.5° S, 170° W) and fig. 1 shows the model horizontal domain. The vertical coordinate, the so-called η coordinate, that represents a generalization of the usual σ coordinate, was introduced in order to reduce

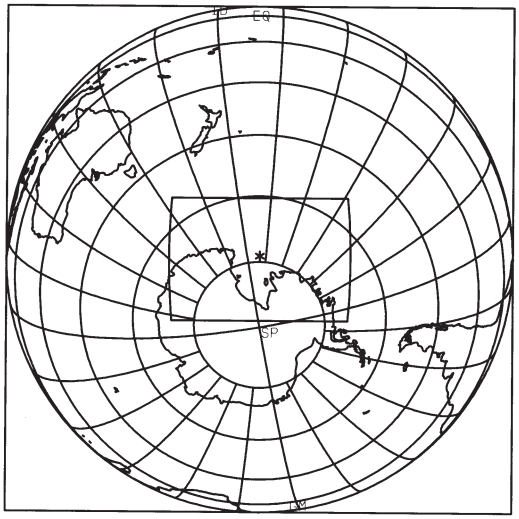

Fig. 1. – Horizontal domain for the ETA simulations. The centre of domain is marked with a star.

problems associated with steeply sloping coordinate surfaces. It is defined by

$$\eta = \frac{p - p_t}{p_s - p_t}\eta_s, \qquad \eta_s = \frac{p_{rf}(z_s) - p_t}{p_{rf}(0) - p_t}, \tag{1}$$

where p is the pressure, z is the geometric height and subscripts t and s denote the values at the top of the model atmosphere and at the Earth's surface, respectively. Here p_{rf} is a suitable defined reference pressure as a function of z (*e.g.*, from polytropic atmosphere). The surface height z_s is allowed to take only a discrete set of values, so that mountains are represented by three-dimensional grid boxes. There are currently 17 levels with highest vertical resolution near the bottom and the top (100 hPa) of the domain. Most prognostic variables are carried out at the middle of each layer. Actual surface elevations are read from US NAVY data 10′ by 10′ resolution, from which the heights of the model mountains are computed. The orography is represented as discrete steps whose tops coincide exactly with model layer interfaces and mountains at six outermost grid point rows of the integration domain are removed [12]. The physical package includes the Mellor-Yamada level 2.5 scheme, the Mellor-Yamada level 2 scheme for the surface layer, used to calculate the turbulence kinetic energy and associated vertical fluxes, the surface process designed following Miyakoda and Sirutis, Betts and Miller cumulus parameterization [15], and the Geophysical Fluid Dynamics Laboratory (GFDL) radiation scheme. The primary prognostic variables in the ETA model are temperature, specific humidity, horizontal wind components, surface pressure and turbulent kinetic energy. The surface temperature, except for ice-free ocean (the sea temperature, SST, is assumed to be constant in time), is also predicted by using an energy balance equation described in detail in [13], given by

$$c_i d_i \frac{\Delta\theta_s}{\Delta t} = FR_n + H_s + H_g + H_w, \tag{2}$$

where c_i is the ice thermal capacity per unit volume, d_i is the soil slab depth, H_s is the sensible heat flux from the atmosphere to the surface, H_g is the sensible heat flux from the layer of the soil to the surface, H_w is the latent heat flux, R_n is the surface net radiation and F is a correction factor which gives the net radiation percent retained in the surface layer. Currently the soil slab depth is 10 cm and the parameter F is prescribed equal to 0.68 when $R_n < 0$ and equal to 0.81 when $R_n \geq 0$ [16]. Sensitivity experiments (not shown) were performed regarding the values of these parameters. The reduction of the soil slab d_i from 10 cm to 2.5 cm, following a suggestion by Janjic (private communication), emphasizes the temporal variation of the surface temperature. When the radiative contribution to the balance equation (1) is increased, setting parameter F equal to 1, the surface temperature tends to be lower than in the control run. In neither experiment, however, the atmospheric circulation shows significant changes. The ECMWF initialized analyses provide initial and boundary conditions for the ETA model runs. The initial conditions refer to 00 UTC 17 February 1988 for this case study and the simulation lasts 48 hours, with a 6-hour update of the boundary conditions. The albedo is set to 0.12 over the sea without ice/snow, 0.60 over sea ice and 0.85 over land with ice/snow coverage. On the basis of literature data we assume that the ocean is covered by ice for latitudes higher than 78° S. On the other hand, the ECMWF analyses show a sea surface temperature less than the freezing point ($T_0 = 271.16$ K) even for latitudes lower than 78° S (see fig. 2). Therefore, in order to have consistent surface fields we assumed that the sea surface temperature over the ice-free ocean cannot be less than T_0. The numerical experiment thus performed is labeled control simulation, CS. The intent here is not necessarily to validate the model

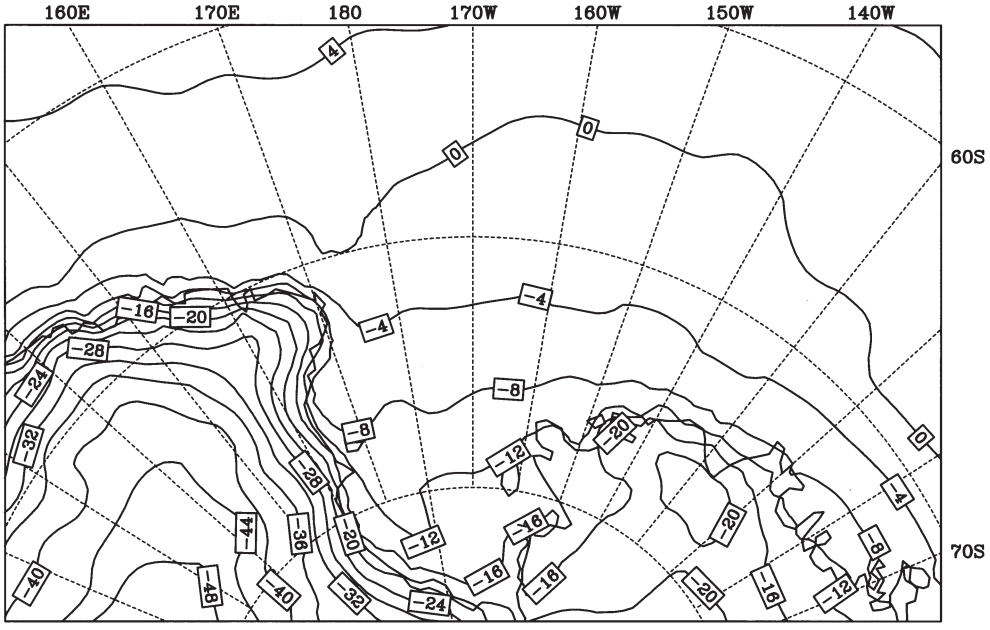

Fig. 2. – ECMWF analysed surface temperature at 00 UTC 17 February. The contour interval is 4° C.

as a forecast tool but, rather, to analyze the development of a mesocyclone off Victoria Land linked with katabatic wind, by using a numerical model. A general overview of the preprocessing and postprocessing characteristics of the ETA model was presented in a previous work [17].

3. – Numerical simulations

3·1. *The synoptic framework.* – In order to assess the synoptic environment that led to the development of the mesoscyclone here investigated, and to point out the differences between the analyses and the simulations, we examined the maps of geopotential height on the isobaric surfaces 850 hPa and 500 hPa relating to 17-18 February 1988. During the period from 00 UTC 17 February 1988 to 00 UTC 19 February 1988, the ECMWF 850 hPa analyses (1.125° horizontal resolution) reveal a low geopotential height zone over the Ross Sea maintaining a cyclonic circulation. Figures 3a) and b) show the ECMWF 850 hPa analyses at 12 UTC 17 February and 18 February. A synoptic cyclone moving eastward is well evident for the whole period. At 00 UTC 18 February, the analyses performed every 6 hours show an increase of the pressure gradient over the southwestern Ross Sea and the subsequent development of a mesoscale cyclone near TNB 12 hours later.

Figure 4 shows the 850 hPa geopotential height field as simulated by ETA for 12 UTC 17 February and 12 UTC 18 February. In this experiment (CS) ETA is run in the full mode, the mountains are represented by the step mountains and the northern limit of the Ross Ice Shelf is set at 78° S. It should be noted that the 850 hPa surface is below the orography over the interior of the continent. The synoptic cyclone slowly moving eastward is reproduced in the simulations, though slightly underestimated and more southwestward at 12 UTC 18 February with respect to the one analyzed in fig. 3. The uncertainly in initial SST as described in sect. 2 could play a role in the observed differences between simulated and analyzed 850 hPa geopotential heights. At this time the mesocyclone just off TNB over the southwestern Ross Sea is reproduced at the development stage. Note that an intensifying trough just off the Victoria Land coast had already been present for several hours before 12 UTC 18 February in the field of 850 hPa geopotential height, probably caused by the shift of air from the continent to the Ross Sea. As was also shown in the meteorological analyses of Carrasco *et al.* [11] using TOVS data, a low slowly moving northward is present on the Ross Ice Shelf, also visible on the 500 hPa isobaric surface. In addition, both 500 hPa analysed and simulated heights reveal a trough over the ocean and a low over Victoria Land moving slowly northeastward (see fig. 5 at 12 UTC 17 February).

3·2. *The mesoscale cyclone.* – Mesoscale and local analyses were performed for the period February 14-20, 1988, using TOVS and AWS observations by Carrasco *et al.* [11]. They show the presence of a permanent subsynoptic scale upper level trough, just off the Victoria Land coast, and the presence of four mesoscale cyclones around TNB; the last and most prominent one occurred at 00 UTC 18 February. They indicate that on this occasion the intense katabatic outflow from TNB is the main factor that induced the formation of the cyclone. In this paper, the purpose of the model run is to capture and examine the developing phase of this vortex. As already mentioned in sect. 2, the simulation starts at 00 UTC 17 February, and at this time the synoptic cyclone already affects the Ross Sea. During 17 February intense easterly and

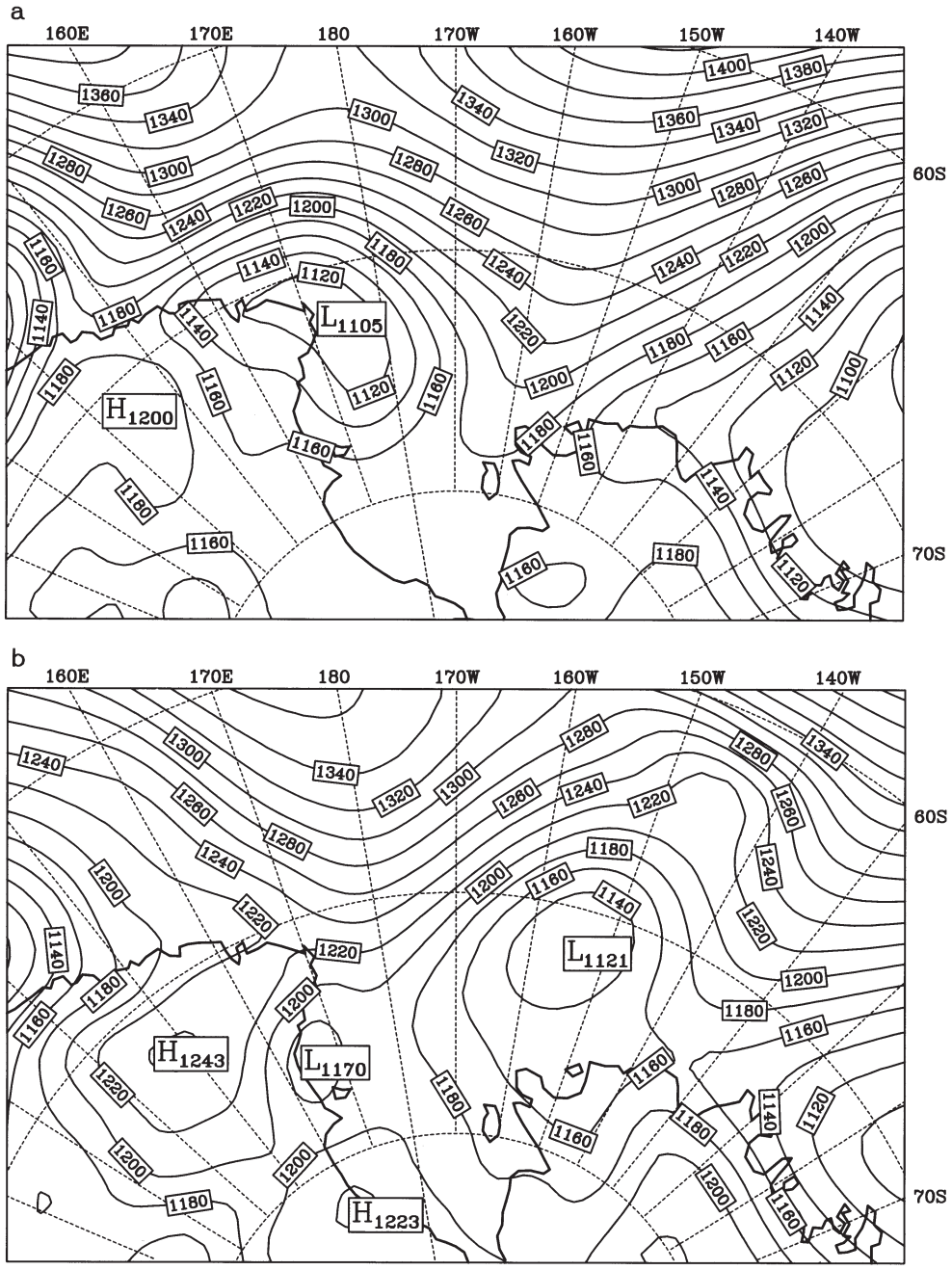

Fig. 3. – ECMWF analyzed for 850 hPa geopotential height. a) 12 UTC 17 February 1988; b) 12 UTC 18 February 1988. The contour interval is 20 gpm.

southeasterly winds are present. They are associated with the synoptic cyclone and move warm maritime air towards Scott Coast and TNB. The wind at first η level above the orography (approximately 300 m above surface over the land and 150 m over the

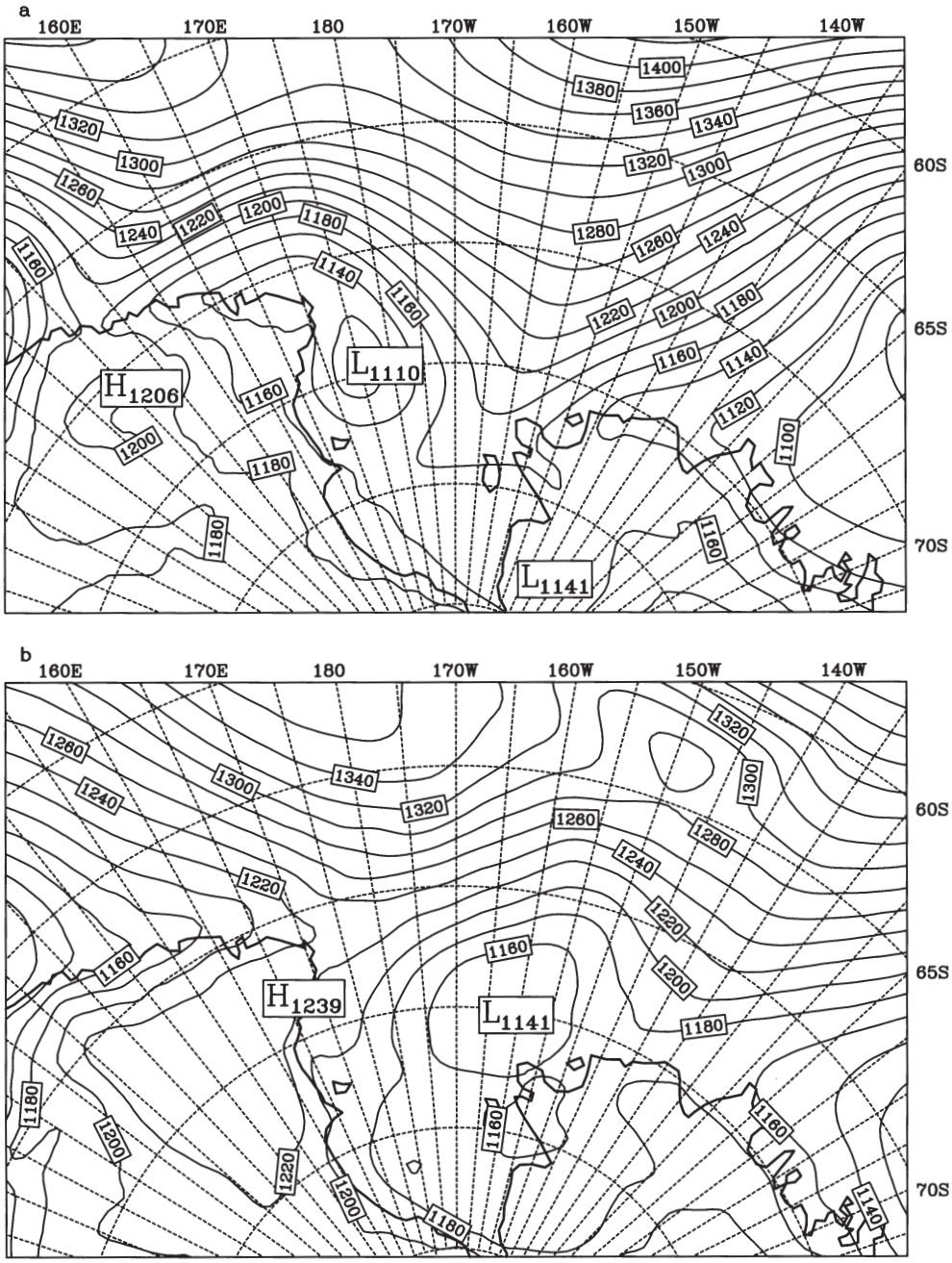

Fig. 4. – Simulated geopotential height at 850 hPa for experiment CS. a) 12 UTC 17 February 1988; b) 12 UTC 18 February 1988. The contour interval is 20 gpm.

Ross Sea) shows that at the initial time and at 06 UTC 17 February over Victoria Land there is no katabatic wind (*i.e.* at TNB the wind blows from the southeast). Six hours later, a cold wind blowing from the southwest is present at TNB, which tends to turn

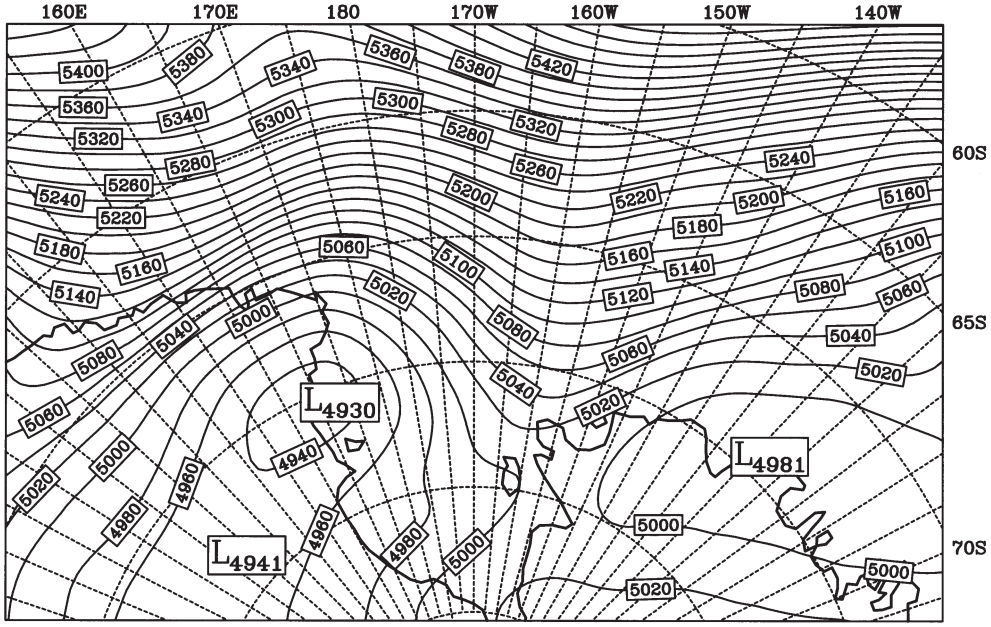

Fig. 5. – Simulated geopotential height at 500 hPa after 12 h time integration. The contour interval is 20 gpm.

further clockwise and to strengthen in the following hours; this clockwise rotation is confirmed by AWS measurements at Inexpressible Island. While the cyclone moves eastward, there is an increase of the sea level pressure gradient inland from TNB associated with the strengthening of the cold orographic wind. Since 06 UTC 18 February a persistent wind blows, with constant direction over Victoria Land towards the coast. At the same time a cold katabatic airstream is forming, coming from the area of Byrd's Glacier, crossing the Ross Ice Shelf and partly mingling with the cyclone flow, partly deflected towards the McMurdo Sound area throughout the second half of 17 February [2]. During the simulation time, the formation of a low-level trough can be noticed in the sea level pressure field, extending approximately parallel to the coast over the western Ross Sea. The wind field at the first η surface above surface, after 36 hours of simulated time (12 UTC 18 February), is shown in fig. 6.

Since the η coordinate surfaces are almost horizontal, for convenience, a composite figure was obtained, in the sense that fig. 6 represents the wind vectors at η levels nearer to the surface. The resolution adopted (about 50 km $\times$ 50 km $\times$ 17 vertical levels) does not enable representation of the fine structures of the orography (see fig. 9b below) or of the effects of channeling of the wind in the TNB area by the Reeves and Priestley glaciers; however, the figure shows that katabatic winds cross the coastline near TNB, while less strong winds, originating from the region north of Byrd's Glacier, blow over the Ross Ice Shelf and enter with the cyclone flow. Over the Ross Sea a deflection of the outflow to the southeast occurs near the coast, caused by the pressure trough parallel to the coast. Wind speeds in the katabatic wind areas are around 10 m/s at about 300 m from the surface. In these areas of fairly strong katabatic winds, the turbulent surface fluxes of sensible heat amount to around -80 W/m^2 and

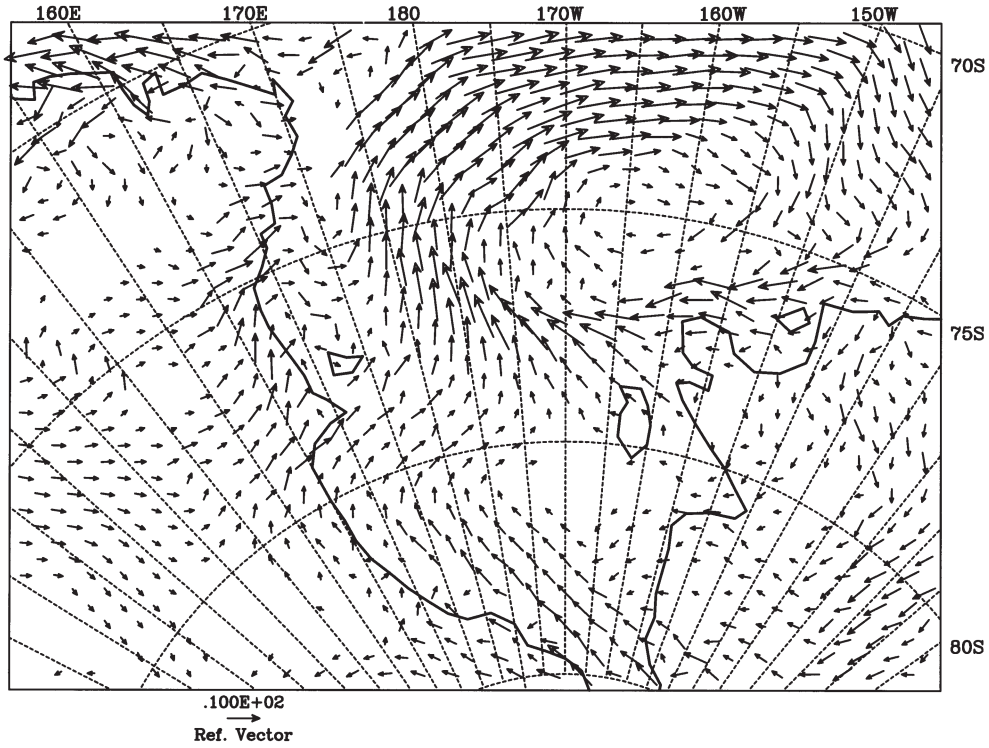

Fig. 6. – Wind vectors at the first η surface in air after 36 h time integration for experiment CS. A scaling vector is shown (ms^{-1}). Vectors whose norm is less than 2 ms^{-1} are not plotted.

-50 W/m^2, while the latent heat fluxes are around 30 W/m^2 and less than 10 W/m^2, respectively. The fluxes of sensible and latent heat over the Ross Sea are positive but their value is around 10 W/m^2 north of Ross Island, probably owing to a simulated weak vertical shear of the wind and the possibly too low surface sea temperature. The thermal contrasts between sea air and katabatic circulation are shown in fig. 7, which represents the potential temperature field after 36 hours of simulated time and at the first η surface in air. For convenience, only a part of the domain is shown. An atmospheric cooling due to advection of cold air is simulated by the model in the TNB coastal area and east of Ross Island, and a narrow zone of higher potential temperature is clearly shown on the Ross Sea. As cited in sect. 2, the SST are constant in the area of study, and thus no temperature gradient is present, except for the one along the coastal areas and at the sea-Ross Ice Shelf interface. At 12 UTC 18 February the pressure at mean sea level shows that a mesocyclone developed north of Ross Island and later is also present at the 850 hPa isobaric surface. Figure 8a shows the pressure field at mean sea level at 18 UTC 18 February, while fig. 8b shows the 850 hPa geopotential height field at the same time.

Comparison between fig. 7 and 8a shows that the position of the mesocyclone corresponds to a zone of fairly high potential temperature; moreover, as revealed by the vertical velocity field (not shown), the katabatic air is characterized by subsidence when it spreads on the ocean, while upward motion is found in the cyclonic vortex [7].

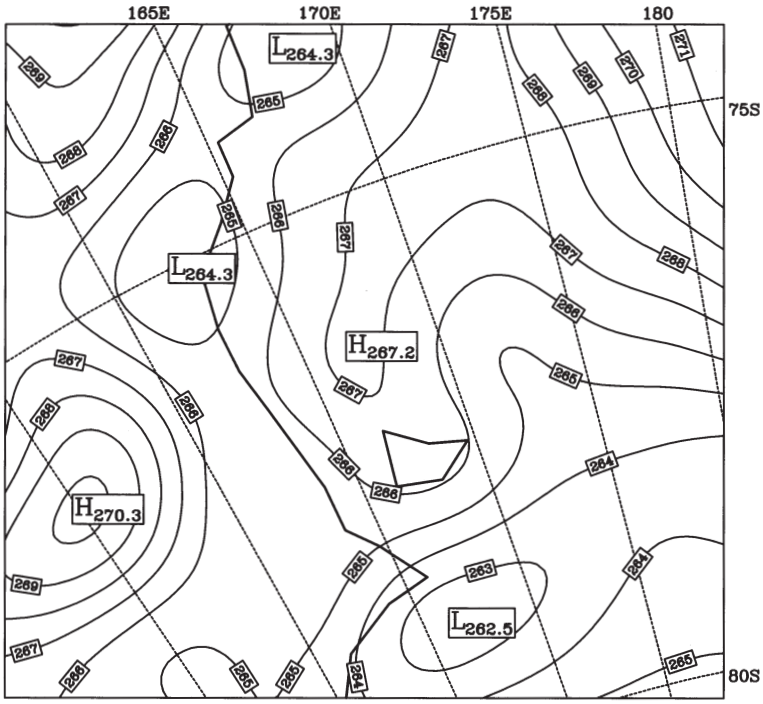

Fig. 7. – Simulated potential temperature at the first η above surface after 36 h time integration for experiment CS. The contour interval is 1K. Only a subsection covering Victoria Land, the southwestern Ross Sea, the northwestern Ross Ice Shelf is shown. (The thick solid line is the coastal line.)

The contrast of pressure at mean sea level between the mesocyclone and the TNB coastline amounts to about 2hPa, as in the meteorological analyses in [11], while on the Ross Ice Shelf southeast of Ross Island the simulated pressure gradient at mean sea level is weaker than in the analyses and is affected by the low on the Ross Ice Shelf visible in fig. 4b. Compared with the ECMWF initialized analyses at the 850 hPa isobaric surface, the mesocyclone that develops in the presence of cold orographic winds is underestimated and grows more slowly. This is probably due to the fact that the speed of the katabatic winds in the TNB area increases more slowly and is lower in the simulation than is necessary. A more detailed wind map at 18 UTC 18 February at the first η surface in air is given in fig. 9a, while fig. 9b shows, for comparison, the AWS observations for the same time and the contours of the step mountains of the ETA model for the horizontal resolution used. The AWS observations show significant differences in both the wind speed and direction, also between near stations, underlining the effects of the orography on a smaller scale than the one used. The speeds of the winds simulated at TNB seem to be too low with respect to those observed, on average, at the AWS stations, though since no vertical interpolation was performed only a qualitative comparison can be made.

3·3. *Idealized simulations.* – The NM experiment differs from the CS one by virtue of the fact that the mountains were zeroed throughout the integration domain.

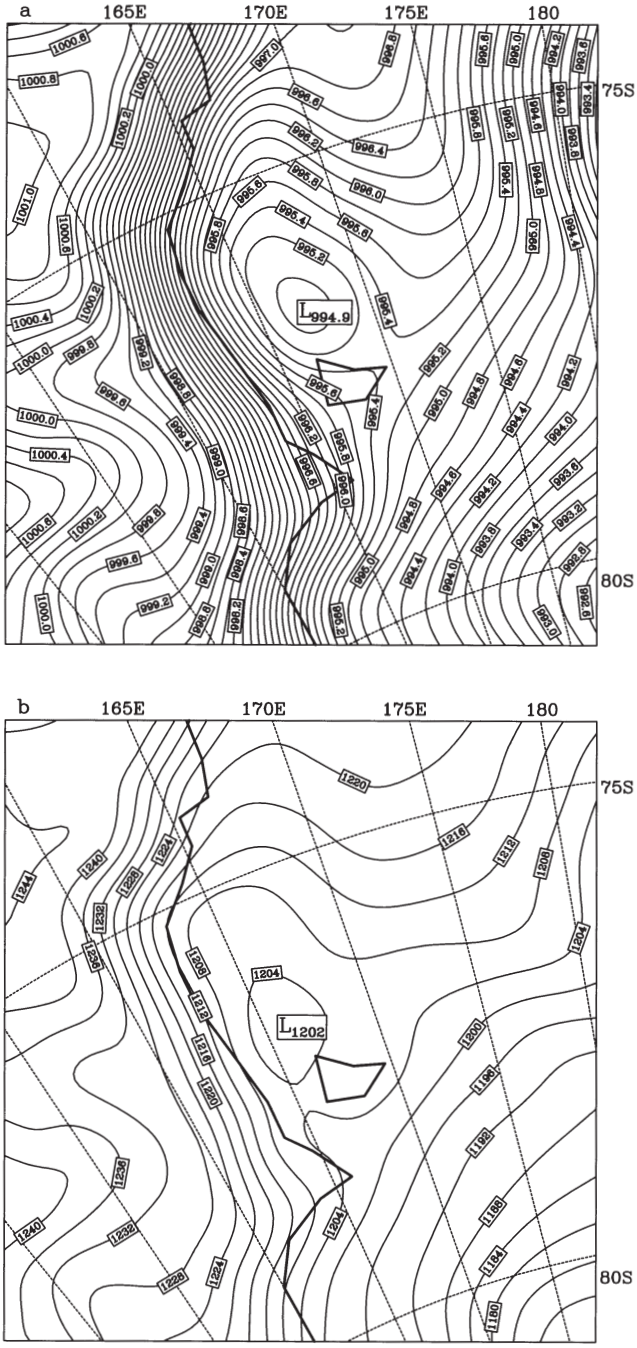

Fig. 8. – a) Sea level pressure (isolines every 0.2 hPa); b) 850 hPa geopotential height (isolines every 4 gpm) at 18 UTC 18 February 1988 for an area as in fig. 7 and for experiment CS.

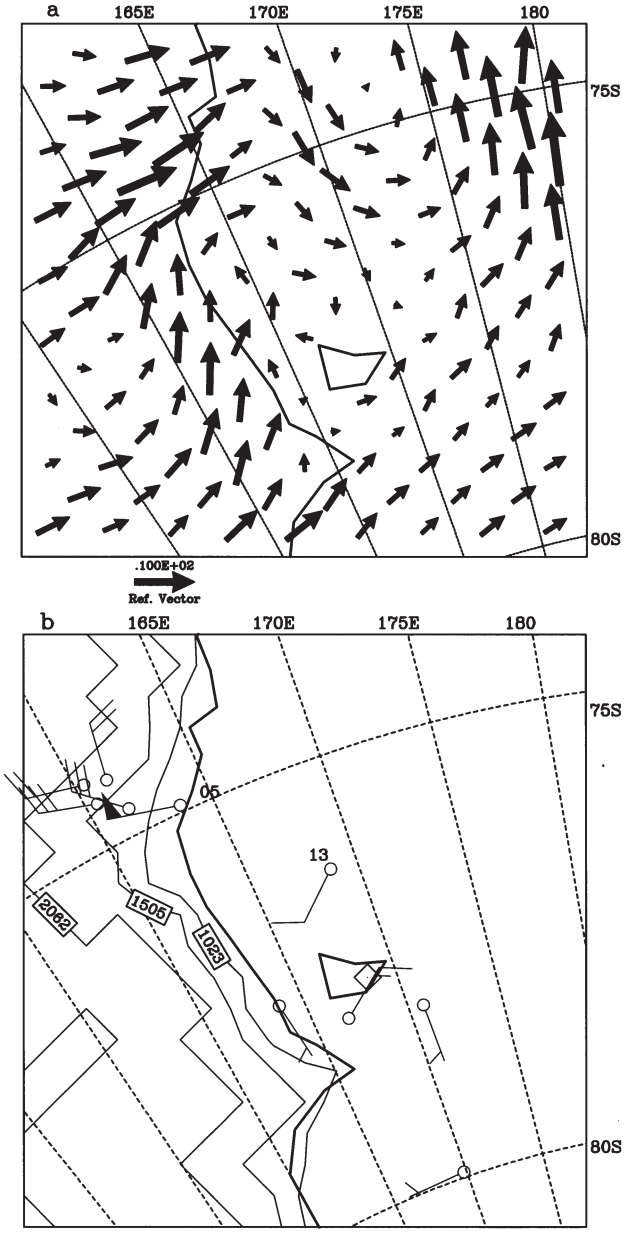

Fig. 9. – a) Simulated wind vectors, a scaling vector is shown (ms^{-1}) at 18 UTC 18 February 1988. Vectors whose norm is less than 1 ms^{-1} are not plotted. b) Step mountains contours and AWS wind barbs at the same time.

Figure 10 shows the geopotential height of the 850 hPa isobaric surface at 12 UTC 18 February.

Comparing the analogous fig. 4b for the CS experiment, it can be noted, in

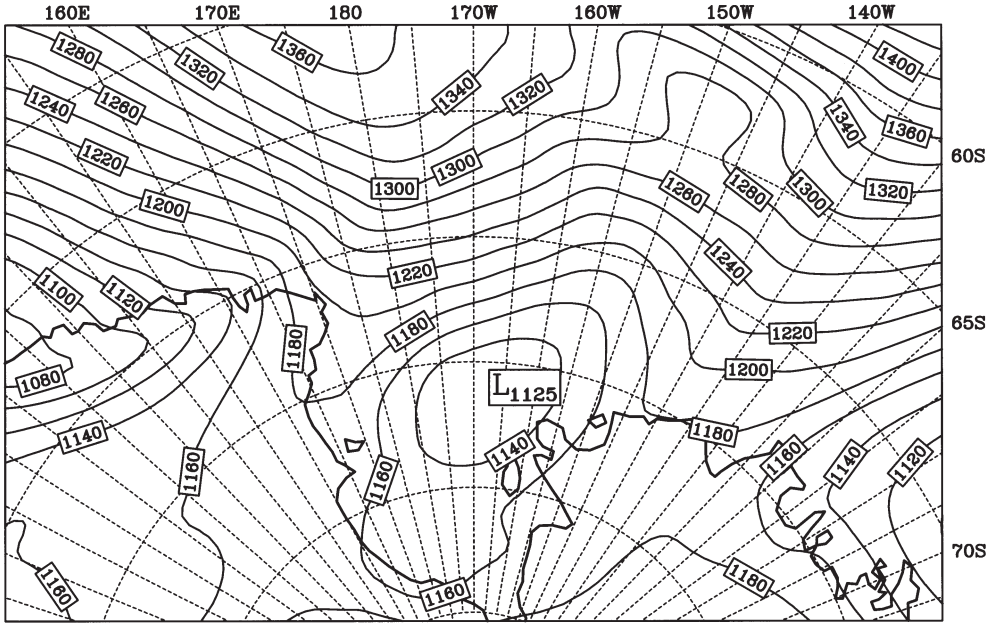

Fig. 10. – Simulated 850 hPa geopotential height at 12 UTC 18 February 1988 for experiment NM. The contour interval is 20 gpm.

particular, that the synoptic cyclone tends to be shifted further southwards and to enter more in the Ross Sea, though its evolution resembles that of the control. Significant differences are present on the southwestern Ross Sea; in this case, no signal of cyclogenesis at the mesoscale is present north of Ross Island. The winds at the lowest η level in this area have an anticyclonic curvature and are directed towards the Plateau (fig. 11). While, on the one hand, this confirms the orographic nature of the CS experiment winds, it underlines, on the other hand, the importance of the cold winds from Victoria Land for the formation of the mesocyclone, that can therefore be classified as a topographically forced mesoscyclone. In the third numerical experiment (SI), we assume that the surface of the ocean is covered with sea ice if the ECMWF sea surface temperature is lower than the freezing point. This means that the ocean surface is covered with ice at latitudes higher than 70° S. Comparison between the SI and CS experiments shows that an ice-covered ocean acts to weaken the synoptic cyclone slightly. In the SI experiment, a trough forms off Victoria Land, both in the geopotential height of the 850 hPa isobaric surface and in the pressure at mean sea level. Figure 12 shows the pressure at mean sea level for the SI experiment at 18 UTC 18 February, and the comparison with fig. 8a reveals the weakening effect of the sea ice on the mesocyclonic activity. The katabatic winds at the coast on the first η surface in air do not undergo significant variations either in speed or in direction with respect to the CS experiment, whereas they slightly decelerate on the ocean (fig. 12b at 18 UTC 18 February) owing to the effect of the different turbulent vertical fluxes of heat at the surface. At 12 UTC 18 February, the surface sensible heat fluxes near TNB and north of Byrd's Glacier are around -80 W/m^2 and -50 W/m^2, respectively, as in the CS

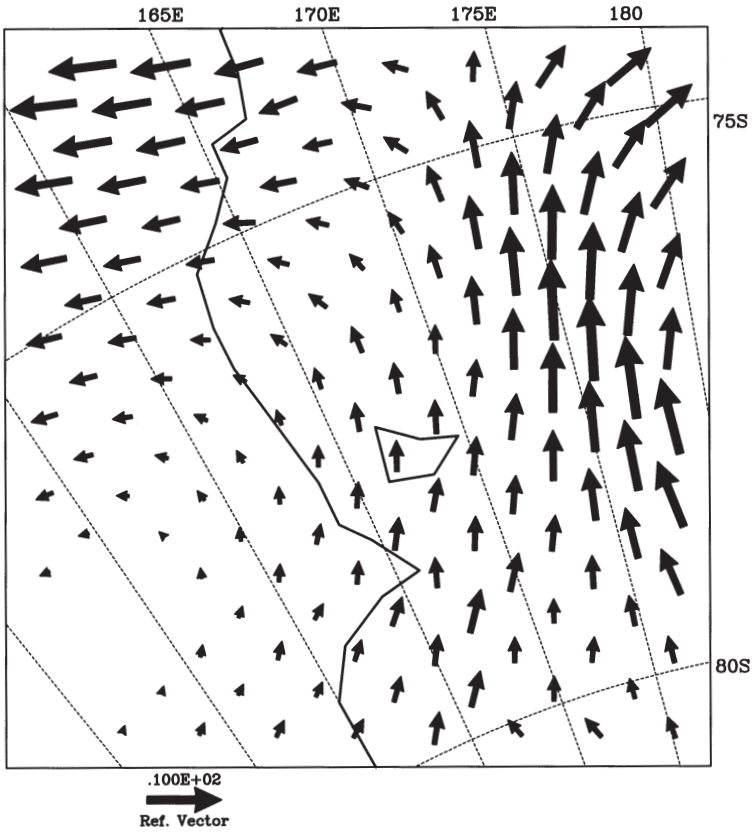

Fig. 11. – Wind vectors at the first η surface in air at 18 UTC 18 February 1988 for experiment NM. A scaling vector (ms^{-1}) is shown and the area is the same as in fig. 7. Vectors whose norm is less than 1 ms^{-1} are not plotted.

experiment, whereas north of Ross Island their value is about -20 W/m^2, revealing a condition of stability at low level. The turbulent vertical flux of latent heat in the area of study and at the same time is significant only on the coast near TNB and amounts to around 30 W/m^2 as in the CS experiment. An additional sensitivity experiment was performed in order to analyze the effect of the sea surface temperature on the development of the mesocyclone. As mentioned in sect. 2, the ECMWF SST turned out to be unrealistic, and therefore in the CS experiment their value was altered so that on the ice-free ocean they should not be lower than $-2°$ C. In this last experiment the SST value increases to 0° C. The trough off Victoria Land forms and the mesocyclone grows more rapidly than in the CS experiment, while, even in this case, the inland circulation at mesoscale and ones at synoptic scale do not undergo large variations. The idealized simulations show that a trough is formed in all the experiments except the NM one, and that the air-sea interaction acts on the deepening and on the temporal growth of the mesolow. For a short simulated time like 48 hours, the inland regime of the katabatic winds and the circulation at synoptic scale due to the nature and thermal characteristics of the sea surface show only minor variations [18].

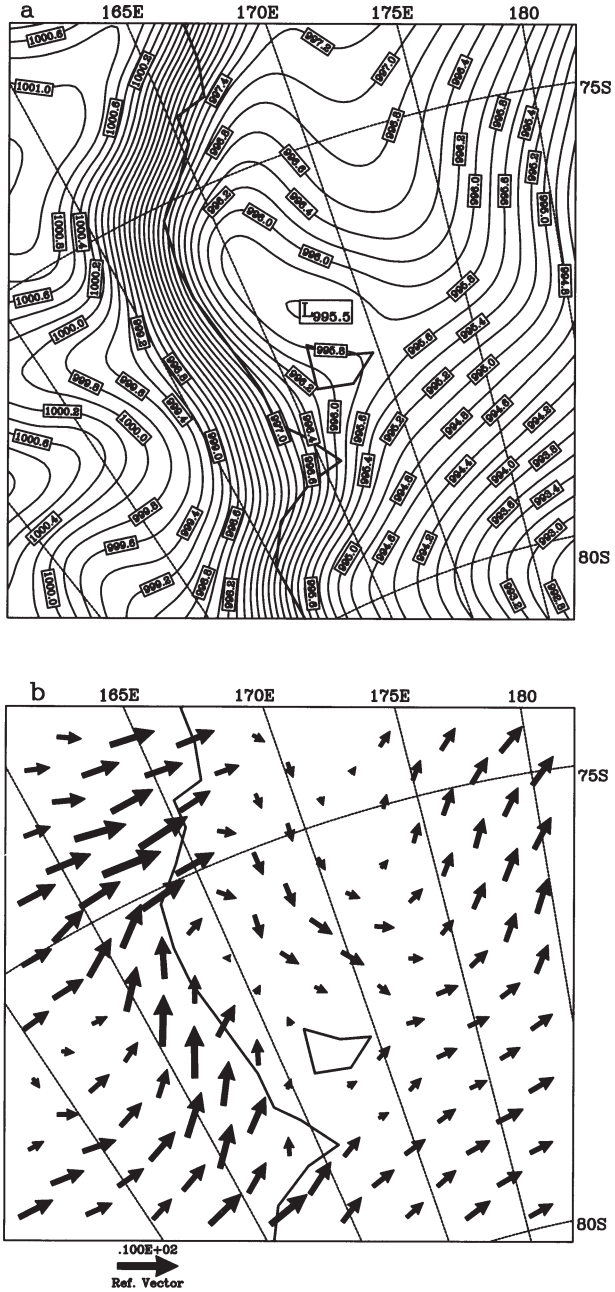

Fig. 12. – a) Sea level pressure (isolines every 0.2 hPa); b) wind vectors at the first η surface in air at 18 UTC 18 February for experiment SI. A scaling vector ms^{-1} is shown and the area is the same as in fig. 7. Vectors whose norm is less than 1 ms^{-1} are not plotted.

4. – Conclusions

The ETA limited area model is used to simulate a real summer event of mesocyclogenesis on the Ross Sea, Antarctica. The initial and the boundary conditions are supplied by the ECMWF initialized analyses. The numerical simulations prove the validity of the ETA model, initialized with ECMWF data for regional studies at high southern latitudes, though the ECMWF analyses seem to present some differences with respect to observations during the period considered. In particular, the surface temperatures of the Ross Sea turn out to be unrealistic. Since the aim of this study is not necessarily to validate the model for prediction purposes but to analyze the characteristics of the simulations and the formation of the mesolow, the results of the ETA model are compared with the ECMWF upper level analyses and, in a limited way, with AWS observations. During the 48 hours of simulated time, a mesocyclone off Victoria Land develops, linked with strong, persisting cold winds from the coast. The simulations show that the ETA model captures many structures at synoptic scale and at the mesoscale in the period 17-19 February 1988, though the simulated mesocyclone turns out to be weaker than the one in the ECMWF analyses. This is connected with the underestimation of the wind speed at low level, that is probably the main shortcoming of the simulation. In the no-mountain experiment throughout the integration model domain, no katabatic wind and no mesocyclone develop, underlining the importance of the orographic forcing. When the ocean is covered with ice, the mesocyclonic activity is weakened, but a trough is in any case present off Victoria Land due to the synoptic environment in combination with the katabatic wind system. For short simulation times like 48 hours the presence of sea ice produces only small variations in the circulation at synoptic scale and in the regime of simulated winds. On the contrary, a surface temperature of the Ross Sea increased by 2 °C tends to strengthen the mesolow and, in particular, to make it grow more rapidly. It is well known that katabatic winds are sensitive to the parametrization of the turbulent fluxes. This suggests that future studies should focus on detailed analysis of the parametrization of the boundary layer fluxes. Lastly, the simulation might be improved by, *inter alia* an increase in the horizontal resolution and, in particular, an increase in the number of vertical layers of the model, with a consequently better resolution of the low atmosphere. Further studies along these lines are being planned.

* * *

This research is supported by the Italian Antarctic Research Programme (PNRA). The University of Modena and Reggio Emilia has allowed a fellowship with PNRA funds. The authors thank A. LAVAGNINI, C. TRANSERICI and the National Meteorological Service of the Italian Air Force.

REFERENCES

[1] HINES K. M., BROMWICH D. H. and PARISH T. R., *A mesoscale modelling study of the atmospheric circulation of high southern latitudes*, *Mon. Weath. Rev.*, **123** (1995) 1146-1165.

[2] SCHWERDTFEGER W., *Weather and Climate of the Antarctic* (Elsevier) 1984.

[3] PARISH T. R., *Surface winds over the Antarctic continent: a review, Rev. Geophys.*, **26** (1988) 169-180.
[4] PARISH T. R. and BROMWICH D. H., *The surface windfield over the Antarctic ice sheets, Nature*, **327** (1987) 51-54.
[5] PARISH T. R. and BROMWICH D. H., *Continental-scale simulations of the Antarctic katabatic wind regime, J. Climat.*, **4** (1991) 135-146.
[6] BROMWICH D. H., *Mesoscale cyclogenesis over the southwestern Ross Sea linked with strong katabatic winds, Mon. Weath. Rev.*, **119** (1991) 1736-1752.
[7] GALLÉE H., *Simulation of mesocyclonic activity in the Ross Sea, Antarctica, Mon. Weath. Rev.*, **123** (1995) 2051-2069.
[8] BROMWICH D. H. and KURTZ D. D., *Katabatic wind forcing of the Terra Nova Bay Polynya, J. Geophys. Res.*, **89** (1984) 3561-3572.
[9] PACCAGNELLA T., PATRUNO P. and CACCIAMANI C., *Operational quantitative precipitation forecast of the Piedmont flood event in the regional meteorological service of Emilia-Romagna, Map Newslett.*, **2** (1995) 7-11.
[10] MARCHESI S., MORELLI S. and STORTINI M., *Intense precipitation as simulated by a limited area model, Phys. Med.*, **XII** (1996) 251-257.
[11] CARRASCO J. F. and BROMWICH D. H., *Mesoscale Cyclogenesis dynamics over the southwestern part of Ross Sea, Antarctica, J. Geophys. Res.*, **98** (1993) 12973-12995.
[12] BLACK T. L., *The step-mountain ETA coordinate regional model: A documentation, NMC notes*, NOAA/NWS/NMC, 1988.
[13] LAZIC L. and TELENTA B., *Documentation of the UB/NMC Eta model, WMO/TMRP Technical Report*, no. **40**, 1990.
[14] MESINGER F., JANJIC Z. I., NICKOVIC S., GAVRILOV D. and DEAVEN D. G., *The step-mountain coordinate: model description and performance for cases of alpine lee cyclogenesis and for a case of an Appalachian redevelopment, Mon. Weath. Rev.*, **116** (1988) 1493-1518.
[15] JANJIC Z. I., *The step-mountain Eta coordinate model: further developments of the convection, viscous sublayer, and turbulence closure schemes, Mon. Weath. Rev.*, **122** (1994) 927-945.
[16] NICKERSON E. C. and SMLEY V. E., *Surface energy budget parameterizations for urban scale models, J. Appl. Meteorol.*, **14** (1975) 297-300.
[17] STORTINI M., MORELLI S. and MARCHESI S., *A first approach on the use of the ETA model in the Antarctic region*, in *Proc. SIF*, edited by M. COLACINO, G. GIOVANELLI and L. STEFANUTTI, vol. **51** (Editrice Compositori, Bologna) 1996, p. 155-159.
[18] PARISH T. R., *On the interaction between Antarctic katabatic winds and tropospheric motions in the high southern latitudes, Austral. Meteorol. Mag.*, **40** (1992) 149-167.